Journal of Geoscience and Environment Protection, 2014, 2, 59-67
Published Online December 2014 in SciRes. http://www.scirp.org/journal/gep
http://dx.doi.org/10.4236/gep.2014.25009

Influence of Fracture Roughness on Aperture Fracture Surface and in Fluid Flow on Coarse-Grained Marble, Experimental Results

G. Dimadis, A. Dimadi, I. Bacasis

Department of Civil Engineering, Laboratory of Technical Geology, Aristotle University, Thessaloniki, Greece
Email: gdimadis@civil.auth.gr

Received October 2014

Abstract

Wetting fluid flow through rock discontinuities influence a great number of project among others: dam construction, underground projects, CO_2 storage in underground schemes, geological disposal of radioactive wastes; Hydrocarbon storage caverns. Flow through fractures is considered to be laminar due to small aperture of the fracture walls and slow velocity. The fluid model called "Cubic law" describes the flow assuming parallel infinite plates. However, natural discontinuities on rock have roughness. In this experimental study an induced fracture on a sample of medium-grained marble was used, to determine the influence of roughness in water flow. This study is a preliminary part of research funding program for flow of CO_2 through rocks (AUTH-GEOMechanics and Environment of CO_2 geological Storage, Project No. 456,400).

Keywords

Cubic Law, Roughness, Hydraulic Aperture, Mechanical Aperture

1. Introduction

In relatively impermeable rocks, the fluid flow is essentially confined in joints and fractures of the rock mass. As a result the hydraulic conductivity of the rock mass is determined by the hydraulic conductivity of joints and fractures. The major factors govern the flow in fractured rocks are, a) fluid properties, b) void geometry and c) fluid pressure at the joint boundary (Olsson & Barton, 2001) (Kranzz, Frankel, Engelder, & Scholz, 1979). Void geometry is ruled by the variation of the aperture between the walls of the fracture and the contact areas (touching asperites) (Zimmerman & Bodvarsson, 1996) which induce the roughness of the fracture walls. In this study the parameter of void space is examined, by testing the effect of joint surface roughness on water flow rate through induced marble fracture.

The relationship between flow rate and hydraulic gradient ($\Delta h/\Delta l$) is given by Darcy's law or so called cubic law Equation (1) (Bear, 1979) (Witherspoon, Wang, Iwai, & Gale, 1980) even though introduced for planar pa-

How to cite this paper: Dimadis, G., Dimadi, A., & Bacasis, I. (2014). Influence of Fracture Roughness on Aperture Fracture Surface and in Fluid Flow on Coarse-Grained Marble, Experimental Results. *Journal of Geoscience and Environment Protection, 2,* 59-67. http://dx.doi.org/10.4236/gep.2014.25009

rallel surfaces should not be generally used to estimate flow through rough surfaces (Oron & Berkowitz, 1998) (Park, Osada, Matsushita, Takahashi, & Ito, 2013; Zhao, Li, & Jiang, 2013; Zimmerman, Al-Yaarubi, Pain, & Grattoni, 2004; Brown, 1987). In conditions that fluid velocity is high and/or joint surface roughness is much, the Cubic Law cannot apply. Moreover it is crucial to calculate the appropriate (most accurate) fracture aperture, so as the predictions of cubic law to be accurate (Renshaw, 1995).

$$Q = \frac{-\rho g}{12\mu} b_h^3 w \frac{\Delta h}{\Delta l} \tag{1}$$

where Q is the flow rate of water passing through two smooth parallel plates, Δh is the difference in hydraulic heads, w is the width of the flowing zone between the parallel plates in the direction normal to the flow vector, Δl is the length of sample, ρ is the fluid density, g is the acceleration due to gravity, μ is the kinematic viscosity of the fluid and b_h is the distance between the two plates (hydraulic aperture).

Roughness affection seems to be in length (Δl). Actually roughness increases the length that fluid has to cover from point A to point B. The longest route causes greater "friction effect" the solids would bring to the fluid, thus decreasing the fracture transmissivity (Bo Li, Jiang, Koyama, Jing, & Tanabashi, 2008). This becomes critical in small joint apertures, because it is translated in greater resistance to flow, and finally in lower conductivity (orders of magnitude) of rough joints (Oron & Berkowitz, 1998)

2. Materials and Method

2.1. Sample Preparation

A sample of marble, of medium-grained Interlocking crystals, with an induced fracture was used in this study. Total dimensions of the samples were: 186 × 45 × 105 mm (**Figure 1**). Artificial fracture was imposed by splitting (tension fracture) one sample in half using custom made metal splitting jaws (a kind of modified "Brazilian" loading method) in a UCS device. A thin scratch in the middle of all surfaces (parallel to the long axis) of the sample was created before splitting, so as to enhance the stress field while loading, as a result almost parallel surfaces of crack occurred.

We studied the influence of fracture roughness on water flow for different joint apertures. Fluid flow is assumed to occur only through the fracture, because the permeability of marble is considered negligible to the joint-flow magnitude.

Eleven hydraulic gradients ($\Delta h/\Delta l$) were selected for each test **Table 1**. It must be mentioned that due to restrictions of the experimental setup in apertures of 750 μm and 1000 μm hydraulic gradients greater than 0.54 and 0.4 respectively, could not be achieved.

Each test concerns the same induced mechanical aperture, six induced mechanical apertures were selected as seen in **Table 2**, these apertures could represent a natural fracture at stage of rest (0 - 500 μm) and stage after shear movement which causes dilation to the fracture surface (>1000 μm) (Yeo, de Freitas, & Zimmerman, 1998).

For each hydraulic gradient we conducted three flow measurements for 50 seconds (after the flow was stabilized) the average flow was calculated. Totally more than 150 measurements were conducted. To ensure that the

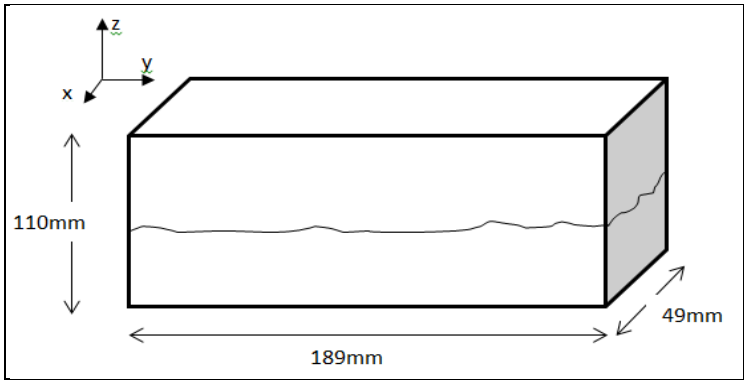

Figure 1. Sample of marble with rough fracture surface.

Table 1. Relation of hydraulic gradient and sample length.

Relation between Hydraulic gradient and Δh/ΔL ratio											
Δh (mm)	2	7.5	15	25	35	50	75	100	125	150	190
Δh/ΔL[1]	0.01	0.04	0.08	0.13	0.19	0.27	0.4	0.54	0.67	0.81	1.02

Note: [1]In our study ΔL is steady (equal to sample length 189mm).

Table 2. Fracture mechanical apertures used in the study.

	Em_1	Em_2	Em_3	Em_4	Em_5	Em_6
Fracture mechanically induced aperture (μm)	0	200	250	500	750	1000

induced mechanical apertures were as accurate as possible, each time we let the sample halves to rest on themselves (Em_1 = 0 μm) and then raised it on the desired aperture. The raise of the upper halve was manually controlled by four linear displacement indicators LDI (Wykeham Farrance, accuracy: ±2 μm) placed at each corner of the sample. For the same aperture to verify reproducibility in measurement at least 3 tests were performed.

2.2. Experimental Set Up

Upper and lower surfaces of the samples were rigidly attached on acrylic plates with dimensions 10 × 65 × 260 mm, 4 thread rods at each corner were used for raising the upper half of the sample on z axis, while 4 Linear displacement indicators were used for exact measurement of level raising, a 5th indicator was used to check for linear movement along x axis. Two smaller acrylic plates with cavities in one side where used as entrance and exit chambers, which allowed water to enter/exit the fracture evenly, minimizing any radial movement.

The hydraulic heads in entrance and exit where measured by two piezometers. Hydraulic gradient was applied each time manually using the piezometers. We employed constant head method by adding a water tank with a spillway to receive constant hydraulic head at specimen entrance, resulting in constant hydraulic gradient throughout each step.

At the exit the spillway of the water tank was used to lead the water coming out of the fracture in a container on a high precision laboratory scale (KERN N2400). Weighting the outcome water gave us the water flow of the crack by using the equivalence 1 ml = 1 g of water. Deaerated water was used throughout the experiment. Total view of the experimental apparatus in **Figure 2**.

To avoid inserting anisotropy in flow as described in Li's study (B. Li, Wong, & Milnes, 2014) due to movement on x axis, 4 rigid metal plates were placed at both sides (y-z planes) of the sample, while raising it on desired mechanical aperture. We used strips of fiber-free elastomeric foam, as no-flow boundary.

2.3. Fracture Roughness Characterization

The sample with the rough faces fracture was scanned with a 3D scan in both faces and the exact micro-topography of the phases was electronically created (**Figure 5**), z axis measurement took place to calculate joint surface roughness.

Characterization of joint surface roughness made by one empirical and one statistical method that are widely used in rock mechanics.

JRC factor (joint roughness coefficient) introduced by Barton (Nick Barton, 1973) is a coefficient used to quantify rock joint roughness, it compares the joint surface duplicate taken with a Profile Gauge Tool for a length of 10 cm, to a table of 10 typical roughness profiles and JRC ranges from 0 (for totally planar faces) to 20 (for very rough surfaces) **Figure 4**. In our case compare of the joints profile gave as an approximation for JRC ≈ 17 (**Figure 3** and **Figure 4**).

The statistical method we used is the dimensionless parameter $Z2$ introduced by Myers (Myers, 1962). It is defined as:

$$Z_2 = \sqrt{\frac{1}{L}\int_0^L \left(\frac{\mathrm{d}y}{\mathrm{d}x}\right)^2 \mathrm{d}x} \tag{2}$$

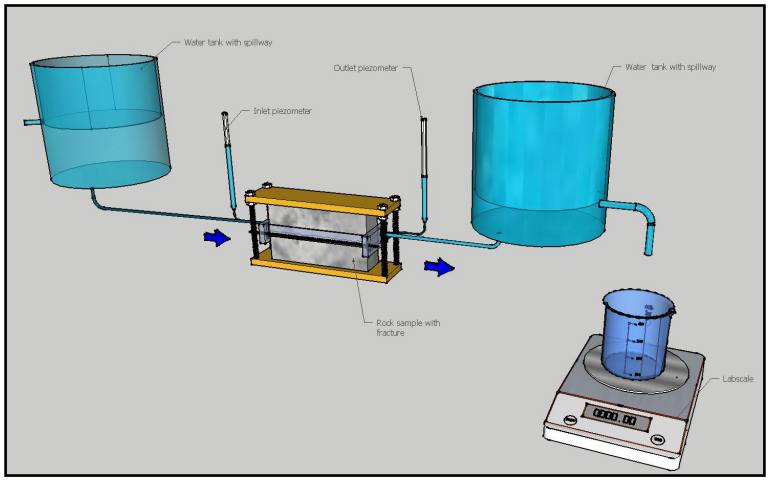

Figure 2. Experimental setup.

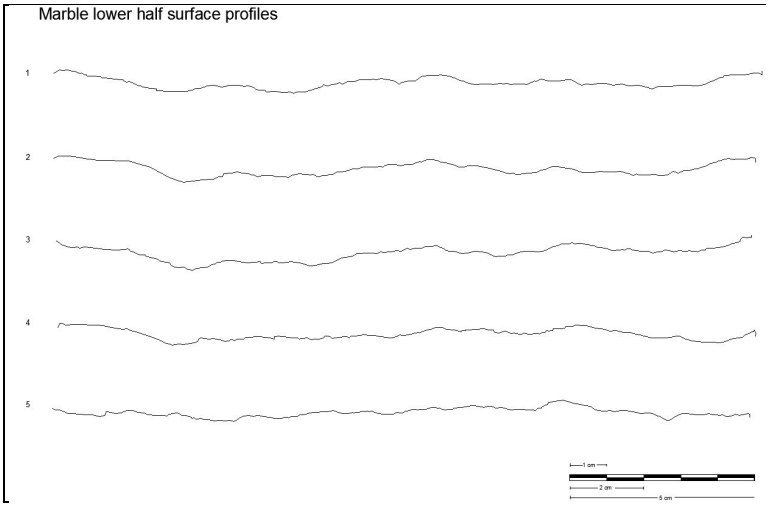

Figure 3. Profiles of lower half taken with profilometer.

where $z(x)$ refers to profile of the fracture surface and L is the profile length. In practice it is calculated by the discretization of the surface profile:

$$Z_2 = \sqrt{\frac{1}{L}\sum \frac{\left(z_{i+1} - z_i\right)^2}{\left(x_{i+1} - x_i\right)^2}} \tag{3}$$

where x_i and z_i the coordinates of the surface profile and L the length of the profile (L = 189 mm).

For the rough fracture surface and 42 profiles along x axis Z2 factor was calculated and JRC coefficient was extracted using Tse's Equation (4) by (Tse & Cruden, 1979). The frequency of JRC results can be seen in **Figure 6.** Mean *JRC* was calculated as 16.38 very close to our approximation (≈17).

$$JRC = 32.2 + 32.47 \log(Z_2) \tag{4}$$

3. Results

The conducting aperture e of the fracture according to Barton (N. Barton, Bandis, & Bakhtar, 1985) is considered identical to parameter b_h of cubic law Equation (1), so after measuring flow rates in our experiment, we back-calculated the conducting aperture that occurred in every flow.

Linear regression between hydraulic gradient and flow rate was observed so laminar flow exists (**Figure 7**).

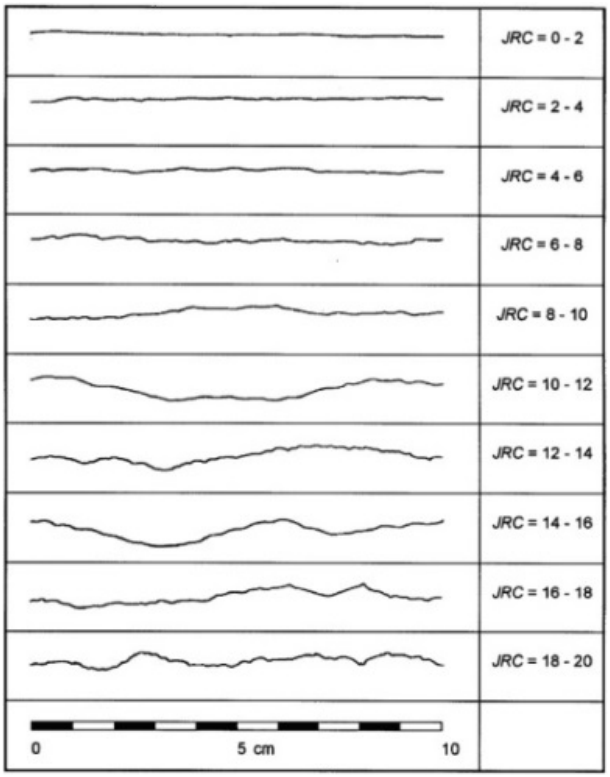

Figure 4. Typical profiles of fractures for JRC coefficient (N. Barton & Choubey, 1977).

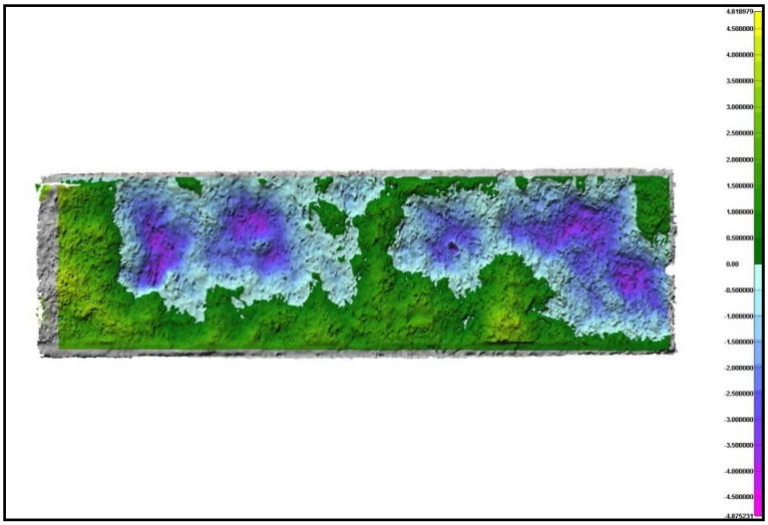

Figure 5. Topography of marble fracture (lower half).

We used the cubic law to back-calculate the hydraulic aperture e (**Figure 8)** for each induced mechanical aperture Em_i 0 μm, 200 μm, 250 μm, 500 μm,750 μm and 1000 μm.

The existence of flow for induced aperture Em_1 = 0 μm (fracture closed under gravity only) and the back calculated hydraulic aperture of 122 μm (**Figure 8(a)**), is incompatible for closed fracture. This indicates that void spaces exist between the two walls of fracture due to roughness and water flows through them.

Using the empirical Equation (5) of Bandis (Bandis, Makurat, & Vik, 1986) for JRC 16.3 and assuming conducting aperture e equal to back calculated hydraulic b_h ($b_h = e$ = 122 μm), the real aperture E is approached as 363 μm (for fracture closed under self-weight).

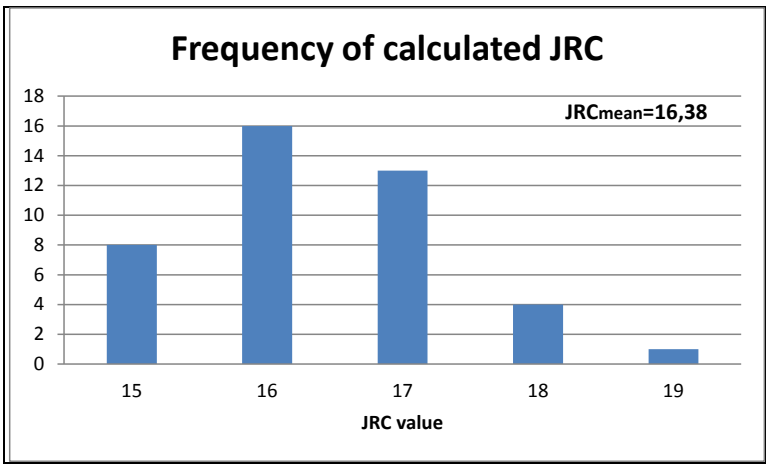

Figure 6. Calculated JRC coefficient for 42 profiles along x axis.

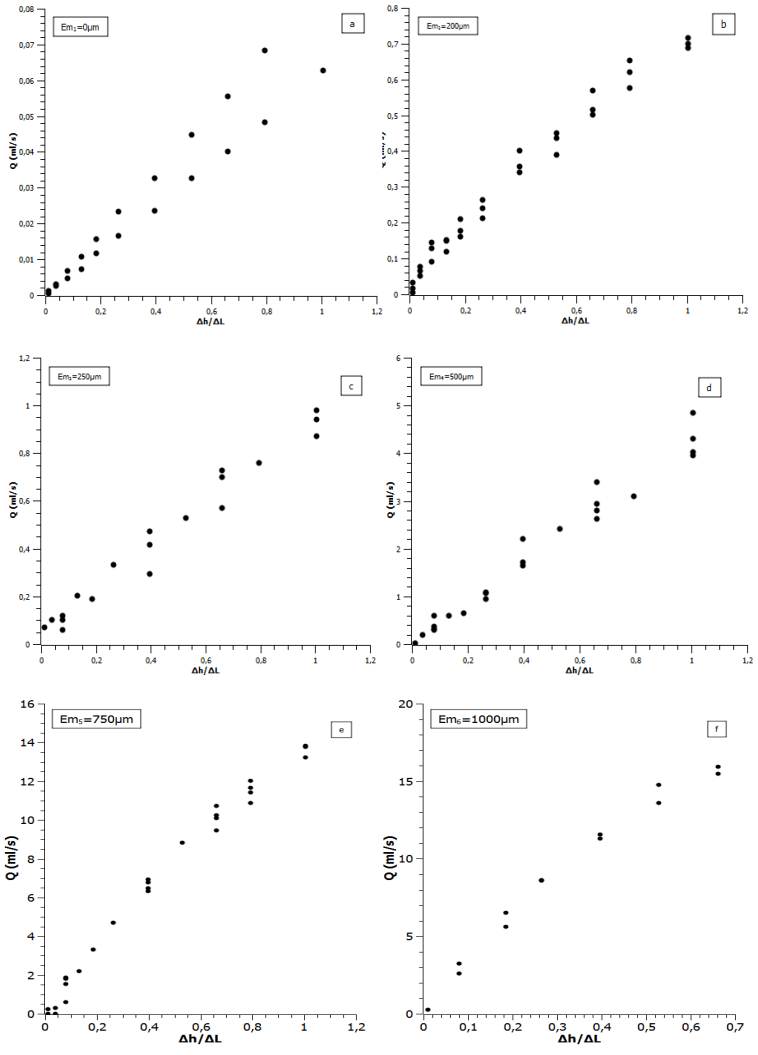

Figure 7. Measured flow rate "Q" for mechanically induced apertures: a) Em_1 = 0 μm; b) Em_2 = 200 μm; c) Em_3 = 250 μm; d) Em_4 = 500 μm; e) Em_5 = 750 μm; f) Em_6 = 1000 μm.

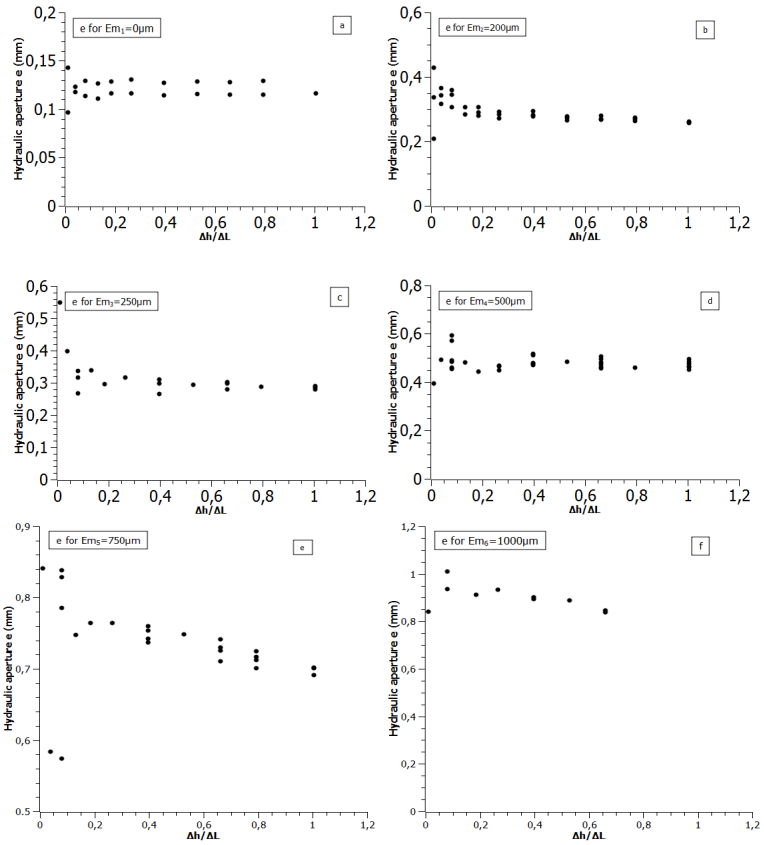

Figure 8. Back calculated hydraulic apertures for mechanically induced apertures: a) Em_1 = 0 μm; b) Em_2 = 200 μm; c) Em_3 = 250 μm; d) Em_4 = 500 μm; e) Em_5 = 750 μm; f) Em_6 = 1000 μm.

$$e = \frac{JRC^{2.5}}{\left(E/e\right)^2}(\mu m) \tag{5}$$

For every mechanically induced aperture the real aperture E was estimated (**Table 3**).

The variation of induced mechanical aperture E_m to real aperture E, is presented in **Figure 9.**

Back calculated hydraulic apertures for mechanically induced apertures: a) Em_1 = 0 μm, b) Em_2 = 200 μm, c) Em_3 = 250 μm, d) Em_4 = 500 μm, e) Em_5 = 750 μm, f) Em_6 = 1000 μm.

4. Conclusions and Discussion

In this preliminary study we tested the influence of roughness and induced aperture on the flow regime by measuring flow rate in a fracture of marble. The roughness of the fracture walls was estimated by the index of *JRC* and factor *Z*2 which gave similar results (JRC ≈ 16.5).

We observed that conducting aperture e (equal to hydraulic aperture b_h which was back calculated by cubic law) and E_m do not coincide, apart from induced aperture Em_6 = 1000 μm. This indicates that cubic law was not valid for apertures lower than 1000 μm.

During the experiment even for E_{m1} = 0 μm flow existed. We calculated the real aperture E using Bandis's Equation (5) which gave E = 360 μm for E_{m1} = 0 μm. Real aperture E became identical to induced aperture E_{mi} only at 1000 μm.

The great differences which were observed between real aperture E and induced aperture E_m indicate that the empirical Equation (5) can be improved.

In our experiment values of conducting aperture, real aperture and induced aperture became identical only at

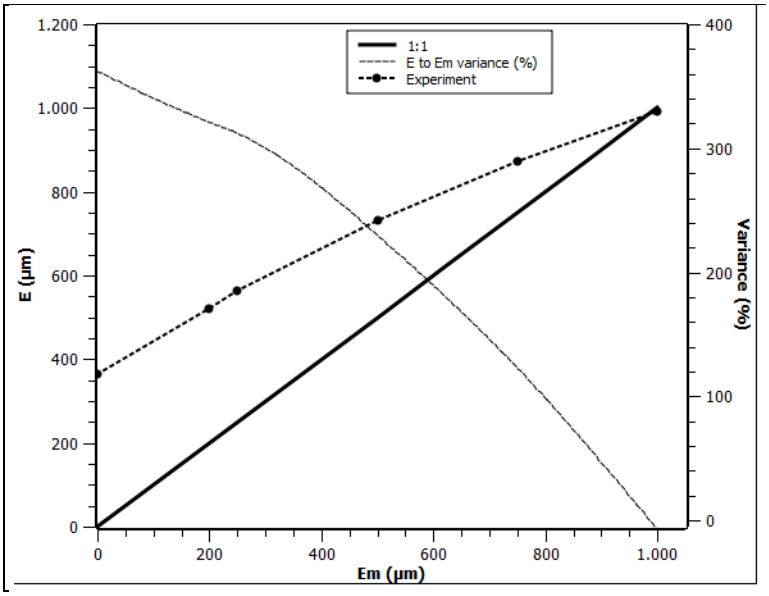

Figure 9. Real aperture *E* to Induced aperture *Em* variation.

Table 3. Estimated real apertures and induced apertures

Induced aperture Em_i	0	200	250	500	750	1000
Back calculated b_h (equal to *e*)	122	250	290	490	700	992
Real Aperture *E*	363	521	562	730	875	1000

1000 μm.

Further tests will take place, in order to approach the relation between induced aperture *Em* and conducting aperture (*e*). Tests will be performed for lower apertures trying to minimize the gap between these two parameters. The value of real aperture for closed fracture (E_0) will be approached by putting the sample under normal stress, further flow tests will take place in these conditions to optimize Bandis' constitutive model (Equation (5)). The same procedure will be followed for samples with different fracture roughness (smooth till very rough).

Later, flow experiments with acid solutions (simulating CO_2-brine conditions under pressure) will be performed, to examine the influence of acidity on fracture roughness and fracture transmissivity.

Acknowledgements

This research has been co-financed by the European Union (European Social Fund–ESF) and Greek national funds through the Operational Program "Education and Lifelong Learning" of the National Strategic Reference Framework (NSRF)-Research Funding Program: Thales. Investing in knowledge society through the European Social Fund.

References

Bandis, S. C., Makurat, A., & Vik, G. (1986). Predicted and Measured Hydraulic Conductivity of Rock Joints. *Publikasjon-Norges Gotekniske Institutt, 164*, 1-11.

Barton, N. (1973). Review of a New Shear-Strength Criterion for Rock Joints. *Engineering Geology, 7*, 287-332. http://dx.doi.org/10.1016/0013-7952(73)90013-6

Barton, N., Bandis, S., & Bakhtar, K. (1985). Strength, Deformation and Conductivity Coupling of Rock Joints. *International Journal of Rock Mechanics and Mining Sciences & Geomechanics Abstracts, 22*, 121-140. http://dx.doi.org/10.1016/0148-9062(85)93227-9

Barton, N., & Choubey, V. (1977). The Shear Strength of Rock Joints in Theory and Practice. *Rock Mechanics Felsmechanik Mecanique Des Roches, 10*, 1-54. http://dx.doi.org/10.1007/BF01261801

Bear, J. (1979). Hydraulics of Groundwater. MacGraw-Hill.

Brown, S. R. (1987). Fluid Flow through Rock Joints: The Effect of Surface Roughness. *Journal of Geophysical Research, 92,* 1337-1347. http://dx.doi.org/10.1029/JB092iB02p01337

Kranzz, R. L., Frankel, A. D., Engelder, T., & Scholz, C. H. (1979). The Permeability of Whole and Jointed Barre Granite. *International Journal of Rock Mechanics and Mining Sciences & Geomechanics Abstracts, 16,* 225-234. http://dx.doi.org/10.1016/0148-9062(79)91197-5

Li, B., Jiang, Y., Koyama, T., Jing, L., & Tanabashi, Y. (2008). Experimental Study of the Hydro-Mechanical Behavior of Rock Joints Using a Parallel-Plate Model Containing Contact Areas and Artificial Fractures. *International Journal of Rock Mechanics and Mining Sciences, 45,* 362-375. http://dx.doi.org/10.1016/j.ijrmms.2007.06.004

Li, B., Wong, R. C. K., & Milnes, T. (2014). Anisotropy in capillary invasion and fluid flow through induced sandstone and shale fractures. *International Journal of Rock Mechanics and Mining Sciences, 65,* 129-140. http://dx.doi.org/10.1016/j.ijrmms.2013.10.004

Myers, N. O. (1962). Characterization of Surface Roughness. *Wear, 5,* 182-189. http://dx.doi.org/10.1016/0043-1648(62)90002-9

Olsson, R., & Barton, N. (2001). An Improved Model for Hydromechanical Coupling during Shearing of Rock Joints. *International Journal of Rock Mechanics and Mining Sciences, 38,* 317-329. http://dx.doi.org/10.1016/S1365-1609(00)00079-4

Oron, A. P., & Berkowitz, B. (1998). Flow in Rock Fractures: The Local Cubic Law Assumption Reexamined. *Water Resources Research, 34,* 2811-2825. http://dx.doi.org/10.1029/98WR02285

Park, H., Osada, M., Matsushita, T., Takahashi, M., & Ito, K. (2013). Development of Coupled Shear-Flow-Visualization Apparatus and Data Analysis. *International Journal of Rock Mechanics and Mining Sciences, 63,* 72-81. http://dx.doi.org/10.1016/j.ijrmms.2013.06.003

Renshaw, C. E. (1995). On the Relationship between Mechanical and Hydraulic Apertures in Rough-Walled Fractures. *Journal of Geophysical Research, 100,* 629-636. http://dx.doi.org/10.1029/95JB02159

Tse, R., & Cruden, D. M. (1979). Estimating Joint Roughness Coefficients. *International Journal of Rock Mechanics and Mining Sciences & Geomechanics Abstracts, 16,* 303-307. http://dx.doi.org/10.1016/0148-9062(79)90241-9

Witherspoon, P. A., Wang, J. S. Y., Iwai, K., & Gale, J. E. (1980). Validity of Cubic Law for Fluid Flow in a Deformable Rock Fracture. *Water Resources Research, 16,* 1016-1024. http://dx.doi.org/10.1029/WR016i006p01016

Yeo, I. W., de Freitas, M. H., & Zimmerman, R. W. (1998). Effect of Shear Displacement on the Aperture and Permeability of a Rock Fracture. *International Journal of Rock Mechanics and Mining Sciences, 35,* 1051-1070. http://dx.doi.org/10.1016/S0148-9062(98)00165-X

Zhao, Z., Li, B., & Jiang, Y. (2013). Effects of Fracture Surface Roughness on Macroscopic Fluid Flow and Solute Transport in Fracture Networks. *Rock Mechanics and Rock Engineering, 47,* 2279-2286 http://dx.doi.org/10.1007/s00603-013-0497-1

Zimmerman, R. W., Al-Yaarubi, A., Pain, C. C., & Grattoni, C. A. (2004). Non-Linear Regimes of Fluid Flow in Rock Fractures. *International Journal of Rock Mechanics and Mining Sciences, 41,* 384. http://dx.doi.org/10.1016/j.ijrmms.2003.12.045

Zimmerman, R. W., & Bodvarsson, G. (1996). Hydraulic Conductivity of Rock Fractures. *Transport in Porous Media, 23,* 1-30. http://dx.doi.org/10.1007/BF00145263